

35 changes in BSA secondary structure were observed at pressure level above 300 MPa,
36 for longer processing times and higher protein concentrations. In these processing
37 conditions β -sheet aggregates were likely to replace the initial α -helices.

38

39 **Keywords:** *High Hydrostatic Pressure, unfolding, aggregation, BSA*

40

41 **1. Introduction**

42 In the last years proteins, the major structural and functional components of several
43 foodstuffs, such as dairy products, meat, bakery products, have been widely
44 investigated, with the aim of formulating novel foods or innovate the texture of
45 traditional foods.

46 The functional properties of proteins, namely physicochemical properties (solubility,
47 binding and surfactant properties, water and oil absorption capacity, emulsifying and
48 foaming properties) influence food preparation, processing and storage, and contribute
49 to the quality perception during food consumption. The exposure of hydrophobic groups
50 on protein surface controls the interactions with oils (emulsions), air (foam) or other
51 proteins (gels and coagula) (Li-Chan & Nakai, 1989). The hydrophobic amino acids are
52 usually buried inside the globular proteins but, as a consequence of the unfolding of the
53 native structure, these hydrophobic groups can be involved in the intermolecular
54 interactions (Kato et al., 1989, Monahan ET AL., 1995).

55 Food processing can affect the functional properties of proteins since it can induce
56 unfolding and aggregation, depending on the technology used, the processing conditions
57 applied and the type of product. The knowledge of the mechanism underlying the
58 structural arrangement of protein molecules may be useful to predict and control protein
59 functionality in food formulations (McClements, 1999). Consequently, processing
60 methods, able to modify the functional properties of proteins, are of interest to the food,
61 chemical and pharmaceutical industries utilizing proteins as functional ingredients in
62 their products.

63 Non-thermal technologies, namely High Hydrostatic Pressure (HHP), Pulsed Light (PL)
64 and Pulsed Electric Fields (PEF), are able to induce changes in functional properties of
65 food protein similarly to the traditional thermal treatments (pasteurization, sterilization).
66 HHP technology is widely applied to inactivate spoiling microorganism and increase the
67 shelf life of foods, preserving their nutritional and sensorial properties. HHP treatments,
68 which have an irrelevant effect on small nutrients, such as vitamins, amino acids and
69 flavour compounds, are instead able to induce changes in macromolecules, mainly
70 proteins and carbohydrates, whose extent is dependent on the treatment temperature, the
71 applied pressure level and the treatment time (Galaska, Dickinson & Ledward, 2000;
72 Barba et al., 2012).

73 HHP processes are able to modify the protein quaternary structure by destroying the
74 hydrophobic interactions, the tertiary structure by reversible unfolding and the
75 secondary structure via irreversible unfolding (Tauscher, 1995). The quaternary
76 structure dissociates at moderate pressures (150–200 MPa), the tertiary structure is also
77 significantly affected at pressure level above 200 MPa and secondary structure changes
78 take place at very high pressure (300–700 MPa) (Ahmed et al. 2010). Protein unfolding,
79 induced by HHP treatments in the pressure range between 100 and 500 MPa, allows the
80 inaccessible SH groups to be exposed. Consequently, the number of the free sulfhydryl
81 (SH) groups and disulfide (SS) bonds also undergo changes during HHP treatments.
82 Under severe processing conditions (above 500-600 MPa, depending on the protein and
83 the temperature applied), the number of free SH group, instead, decreases, probably due
84 to the formation of disulfide bonds by oxidation, especially at alkaline pH where the
85 thiolate anions are more reactive. For instance, the SH-SS interchange reactions induced
86 by HHP treatments were observed for β -lactoglobulin by Funtenberg (1995). The high
87 degree of exposure of sulfhydryl groups, and the subsequent oxidation and sulfhydryl-
88 disulfide bond exchange reactions result in insoluble and/or soluble aggregates and gel
89 formation. Tang & Ma (2009), who investigated the occurrence of aggregates formation
90 in soy protein isolate (SPI) treated by HHP processes at 200–600 MPa, observed
91 combined insoluble (IA) and soluble (SA) aggregates. The relative ratio of IA and SA
92 aggregates depended on the pressure levels. At pressure level above 200 MPa, more
93 soluble aggregate were formed at the expense of insoluble aggregates (Tang & Ma,
94 2009). Soluble aggregates were also observed for β -conglycinin and glycinin treated at
95 pressure levels between 300-600 MPa (Speroni et al., 2009). Similarly HHP promoted
96 aggregation and significantly increased the surface hydrophobicity of Rapeseed Protein
97 Isolates (RPI) (Rong et al., 2013).

98 The number of the disulfide bonds, moreover, affects the texture of the HHP induced
99 gels, being the storage modulus, related to the elasticity of a solid, proportional to the
100 cross-linking density in the gel network (Qin et al., 2012).

101 HHP treatments affect also the proteins functional properties: the viscosity and the
102 surface tension are increased, as observed for egg white (Yang et al., 2009) and the
103 foaming capability is increased, as demonstrated for ovalbumin (Denda & Hayashi,
104 1992) and egg white (Knorr et al., 1992; Yang et al., 2009). Yang et al. (2009) observed
105 a direct correlation between the egg white foaming ability and the number of free SH

106 groups. At the lowest hydrophobicity level of egg white foaming capacity and foam
107 stability of egg white reached the maximum value (Yang et al., 2009).

108 The changes of functional properties as well as the variation of the conformational
109 structure may be particularly relevant in case of allergens, which are mainly specific
110 glycoproteins able to activate the reaction of the human immune systems (Gross, M. &
111 Jaenicke, 1994; Penãs, et al., 2006; Shriver et al., 2010). Bovine Serum Albumin (BSA),
112 a globular protein soluble in water, represents a very interesting case of investigation,
113 being a protein component of whey and blood and a common allergen of bovine meat
114 and whey proteins. Moreover BSA physicochemical and structural properties have been
115 investigated and measured, making it a desirable model for the research on food protein.
116 BSA is a protein responsible for several allergic cross-reactions: most children with
117 beef allergy are also allergic to cow's milk and should avoid the consumption of dairy
118 products. Sensitization to bovine serum albumin is a marker of cow's milk allergy in
119 children with beef allergy (Martelli et al., 2002). Furthermore, cooking or other
120 processing methods do not necessarily eliminate the allergenic epitopes from milk and
121 meat products. Nevertheless few papers, which investigated the effects of HPP
122 processing on BSA, demonstrated that the solution properties of the protein can be
123 affected by pressure (Buckow et al., 2011).

124 According to these findings, this paper proposed an extensive characterization of a HHP
125 treated allergenic protein, Bovine Serum Albumin (BSA), with the aim of individuating
126 the mechanism of action of HHP technology on the structure as well as on the
127 functional and biological properties of this compound and determining to which extent
128 the physical and structural changes occurring to the proteins previously described can
129 be observed for this particular case. An extended experimental campaign was carried
130 out to assess the effects of HHP process parameters, namely pressure level and time,
131 and protein concentration on the structural characteristic of the allergens.

132 The effect of processing conditions, namely pressure level and treatment time, on the
133 conformational structure and the functional properties of BSA solubilized in a buffer
134 solutions at different concentration in buffer solution was analyzed. BSA unfolding and
135 refolding were analyzed in terms of free sulfhydryl (SH) groups, changes of secondary
136 structure, foaming and emulsifying properties. The experimental data were analyzed in
137 order to identify the role of the process parameters in the transition from reversible
138 unfolding to irreversible unfolding/aggregation of this protein. A deeper understanding

139 of the mechanisms governing the conformational changes will be very useful to design
140 novel processes addressed to the reduction and/or elimination of food allergenicity.

141

142 **2. Materials and Methods**

143 **2.1 Preparation of the samples**

144 Different amount of BSA protein (Sigma-Aldrich, Italy) to reach the concentration of 50
145 and 100 mg/mL was dissolved, at a temperature of 25 °C, in Sodium Phosphate Buffer
146 (50 mM, pH=8), according to the protocols reported by Penãs et al. (2006). After a
147 gentle mixing, a homogenous solution was obtained. The pH of the protein solution was
148 measured with a pH-meter (S400 SevenExcellence, Mettler Toledo International Inc.).
149 The protein solutions were stored under refrigerated conditions before HHP treatments.

150

151 **2.2 Experimental Apparatus**

152 The HHP system U22 (Institute of High Pressure Physics, Polish Academy of Science,
153 Unipress Equipment Division, Poland), which is a laboratory scale unit provided with a
154 vessel which has a maximum processing volume of 50 mL, was used during the
155 experiments.

156 The system can be operated in a wide pressure range (0 - 1400 MPa) under thermal
157 controlled conditions (25 - 120 °C).

158 Operating pressure, ramp rate and processing time are set up on a control panel, which,
159 in turn, allows the opening and the closure of the HHP vessel. A portable Temperature
160 Power and control Unit (TCU) connected to the main unit with electrical cables and
161 thermocouples (K-type) permits the set up and control of the operative temperature in
162 the HHP vessel. The vessel is heated with electrical heaters and cooled with compressed
163 air. The pressurizing medium is Plexol (Bis (2-ethylhexyl) sebacate from Sigma-
164 Aldrich, Italy) and the estimated temperature increase due to pressure build-up is 2-3
165 °C/ 100 MPa.

166

167 **2.3 Experimental plan**

168 **2.3.1 Experimental protocols**

169 For the experimental campaign 5 mL of BSA solution were sealed in flexible pouches
170 made of a multilayer film (Polyethylene-Aluminium-Polypropylene). The pouches were
171 introduced into the U22 vessel and the pressure cycle set at the desired processing

172 conditions. All tests were carried out at ambient temperature (25 °C), while the
173 operating pressure was varied in the range between 100 and 600 MPa, and the operating
174 time between 15 and 25 min. After the pressure release, the pouches were collected
175 from the vessel, dried with blotting paper and stored at 4 °C before undergoing chemical
176 characterization. All experiments were conducted in triplicate.
177 SH free groups, foaming properties, FT-IR spectra, and emulsifying properties were
178 determined on unprocessed and processed samples according to the protocols reported
179 in the following paragraphs.

180

181 **2.3.2 Determination of free SH groups**

182 Free sulfhydryl (SH) groups of BSA samples were evaluated according to the protocols
183 reported by Beveridge et al. (1974) and by Hardham (1981). Ellman's reagent was
184 prepared by dissolving 4 mg of 5,5-dithio-bis 2-nitrobenzoic acid (DTNB) (Sigma-
185 Aldrich, Italy) in 1 mL of Tris-Glycine buffer (0.1 M Tris-(hydroxymethyl)-
186 aminomethane (Tris), 0.1 M glycine, and 4 mM ethylenediamine-tetraacetic acid
187 disodium salt, pH=8.0; Sigma-Aldrich, Italy)). BSA (10 mg), dissolved in 5 mL of 8M
188 urea in Tris-Glycine buffer, was added to the Ellman's reagent (40 µL) and incubated
189 for 30 min at room temperature (25 °C). The absorbance was measured at 412 nm with
190 a UV/VIS spectrophotometer (V-650, Jasco Europe Srl, Italy), using Tris-Glycine
191 buffer as blank. Free sulfhydryl groups were evaluated according to Equ.1:

192

$$193 \quad \text{SH}(\mu\text{M/g}) = 73.53 * A_{412} * D/C \quad (1)$$

194

195 being A_{412} the absorbance at 412 nm, C the sample concentration in mg solid/mL and D
196 the dilution factor. Results were expressed as the mean of three measurements.

197

198 **2.3.3 Determination of FT-IR spectra**

199 The secondary structure of the BSA samples was determined with a FT-IR
200 spectrophotometer (FT-IR-4000, Jasco Europe Srl, Italy) at ambient temperature (25
201 °C). BSA samples (50-100 mg/mL) were dissolved in Sodium Phosphate Buffer (pH=
202 8) and treated under HHP (pressure level=100-600 MPa; treatment time=15, 25 min).
203 For each test the transitions among different vibrational energetic levels were recorded
204 in terms of absorbance spectra as a function of the measurement time.

205 The Fourier Transform was applied to the recorded spectra in order to observe the
206 behavior of the absorbance values as a function of the frequency (wavelength factor,
207 cm^{-1}). The second derivative and Fourier self-deconvolution were applied to the infrared
208 spectra.

209

210 **2.3.4 Determination of the foaming properties**

211 The foaming properties of BSA solutions untreated and treated under HHP (P=100-600
212 MPa; t=15, 25 min) were determined according to the protocol of Hammershoj and
213 Larsen (1999) reported by Lomakina et al. (2006). A volume of 5 mL of the sample was
214 placed in a glass beaker of 100 mL and stirred at 18000 rpm for 5 minutes at ambient
215 temperature (25 °C). The produced foam was gently transferred into a graduated glass
216 cylinder (diameter= 2 cm, height=16 cm, graduated volume= 25 mL) to determine the
217 foam volume (V_f). The Foaming Capacity (FC) was calculated as the ratio between the
218 measured foam volume (V_f) and the initial volume of liquid solutions (V_0), according to
219 Equ. 2:

220

$$221 \quad \quad \quad \text{FC} = V_f/V_0\% \quad \quad \quad (2)$$

222

223 The results were expressed as the mean value of three independent measurements.

224

225 **2.3.5 Determination of turbidity, emulsifying activity and emulsion stability**

226 Turbidity, Emulsifying Activity Index (EAI) and Emulsion Stability Index (ESI) of the
227 protein solutions were determined according to the turbidimetric method developed by
228 Pearce and Kinsella (1978), and modified by Tang et al. (2005) and Yang et al. (2010).

229 6 mL of BSA protein solution (50-100 mg/mL in Sodium Phosphate Buffer (50 mM,
230 pH=8)) and 2 mL of peanut oil were homogenized in a high-speed homogenizer (T-25
231 ULTRA-TURRAX Digital Homogenizer, IKA®-Werke GmbH & Co. KG) for 1 min at
232 10.000 rpm. A 50- μL emulsion was taken at different times from the bottom of the
233 homogenized emulsion, and diluted (1:100) in a sodium dodecyl sulfate (SDS) 0.1%
234 (w/v) solution.

235 After the diluted emulsions were shaken in a vortex mixer for a moment, the absorbance
236 was read at 500 nm against a blank (dilution solution) in a UV/VIS spectrophotometer
237 (V-650, Jasco Europe Srl, Italy).

238 The EAI was calculated using Equ. (3), proposed by Cameron et al. (1991) and adopted
239 by Silva et al. (2003) and Tang et al. (2005):

240

$$241 \quad EAI \left(\frac{m^2}{g} \right) = 2 * \frac{T}{[(1-\theta)*C*1000]} \quad (3)$$

242

243 where T is the turbidity, θ is the fraction of oil used to form the emulsion (0.25) and C is
244 the initial concentration of protein (5-10 g/100 mL). The turbidity was calculated using
245 Equ. (4):

246

$$247 \quad T = 2.303 * \frac{A*DF}{OP} \quad (4)$$

248

249 where A is the absorbance of the sample at 500 nm, DF is the dilution factor (100) and
250 OP is the optical path (0.01 m).

251 The ESI was measured according to the method described by Chobert et al. (1988) and
252 adopted by Silva et al. (2003), with a minor modification. The $\Delta EAI\%$ was calculated
253 according the Equ. (5):

254

$$255 \quad \Delta EAI\% = \frac{(EAI_{MAX} - EAI_{MIN})}{EAI_{MAX}} * 100 \quad (5)$$

256

257 where EAI_{MAX} is the highest value of EAI obtained for the diluted emulsions right after
258 their formation, and EAI_{MIN} is the value obtained from the emulsion after storage for 10
259 min.

260 The values of ESI were calculated using Eq. (6):

261

$$262 \quad ESI = 1/\Delta EAI\% \quad (6)$$

263

264 The results were expressed as the mean value of three independent measurements.

265

266 **2.4 Statistical analysis**

267 The experiments were carried out in triplicate (3 independent runs) and the standard
268 deviations of the results were calculated and reported.

269 The analysis of variance test for significant effects of treatments and assay samples
270 were determined using the SPSS Statistics software. Experimental data were statistically

271 analyzed performing an analysis of variance (two-way ANOVA). Main effect
272 differences were considered significant at the $p < 0.05$ level.

273 The Pearson product-moment correlation coefficient was used to measure the strength
274 of the linear relationship between two variables.

275

276 **3. Results and discussion**

277 **3.1 Effect of HHP treatments on free SH groups**

278 Most of the free SH groups in the native globular proteins are masked to the attack by
279 Ellman's reagents, due to their location in poorly accessible regions of the polypeptide
280 chain. The application of an external agent, such as temperature and/or pressure,
281 modifies the protein conformational structure with the consequent unmasking and
282 activation of SH groups, which can be detected according to the protocol of the
283 Ellman's reaction (Beveridge et al., 1974; Hardham, 1981). Therefore the analysis of
284 the free SH-groups may be considered as an indication of protein unfolding and/or
285 denaturation.

286 The concentration of free SH groups in the BSA samples (50 and 100 mg/mL) treated at
287 pressure levels from 100 to 600 MPa for 15 and 25 min was estimated. In Figure 1 the
288 experimental data obtained according to the protocol based on Ellman's reagents are
289 reported. The concentration of free SH groups in the native protein solutions is around
290 0.27 $\mu\text{mol SH/g}$.

291 The effect of HHP treatments on the concentration of free SH groups depends on the
292 processing conditions (pressure level and holding time) as well as on the BSA
293 concentration in the processed protein solutions.

294 In BSA samples with a concentration of 50 mg/mL the number of free thiol groups
295 increases with the pressure level up to a threshold value, which depends on treatment
296 time and protein concentration in the solution. According to the experimental data
297 plotted in Figure 1A, the value of the threshold pressure is 400 MPa for a treatment time
298 of 15 minutes and 300 MPa about for a treatment time of 25 minutes. The number of
299 SH groups estimated for the samples treated at the same pressure level decreases with
300 prolonging the processing times, which, similarly to pressure level, contribute to
301 anticipate aggregation phenomena in protein solutions.

302 Above the defined value of the threshold pressure, the dependence of the number of free
303 SH groups on pressure level follows an opposite trend. Experimental data demonstrate

304 that, similarly to temperature, high hydrostatic pressure is able to induce protein
305 unfolding, which allows the masked SH groups to be exposed and consequently
306 detected. However, under pressure the unmasked SH groups are more reactive and
307 above the threshold pressure level the decrease in total SH content could be due to the
308 sulfhydryl-disulfide bond exchange reactions, which are especially promoted at alkaline
309 pH. Similarly Qin et al. (2012) detected a higher number of SH groups in the pressure
310 range between 300-400 MPa and their significant decrease in the pressure range of 400-
311 500 MPa probably due to the formation of aggregates (Quin et al., 2012). Van der
312 Plancken et al. (2005), who studied the effect of heating and high pressure treatments on
313 egg white proteins, observed the exposure of buried SH groups and the formation of
314 aggregates at pressure levels of 500-600 MPa with a consequent decrease in free SH
315 content due to the oxidation of the thiols and the formation of disulphide bonds.

316 The experimental data reported in Figure 5.2 demonstrate the relevant role of protein
317 concentration in determining the effect of HHP treatment on the conformational
318 structure of BSA. As already observed at lower BSA concentration, the number of free
319 SH groups in the HHP treated samples is higher than in the native protein solution.
320 However, if the data of BSA samples with protein concentrations of 50 mg/mL and 100
321 mg/mL are compared, higher protein concentrations reduce the number of free SH
322 groups detectable.

323 This result can be explained by hypothesizing a different mechanism governing the
324 protein behavior under pressure rather than a reduced efficacy of the HHP treatment in
325 unmasking the buried SH groups. The availability of free SH groups unmasked under
326 pressure and of more contact points due the high protein concentration in solution
327 enhance the protein-protein interaction and the formation of both short and long terms
328 bindings between neighboring polypeptide side chains (Cheftel et al., 1985). In fact,
329 samples with protein concentration of 100 mg/mL have a lower number of free SH
330 groups, due to the aggregation phenomena which already occur at pressure level of 300
331 MPa. In this case prolonged holding time do not have any significant effect on this
332 parameter ($p < 0.05$), while pressure levels above 300 MPa determine a slight increase of
333 the number of free SH groups, thus demonstrating a progressive modification of the
334 conformational structure of the pressure-induced aggregates.

335

336 **3.2 Effect of HPP on secondary structure of BSA**

337 **3.2.1 FTIR spectrum of BSA at ambient temperature**

338 FT-IR spectroscopy, unlike X-ray crystallography and NMR spectroscopy, provides
339 information about the secondary structure content of proteins in water solutions as well
340 as in deuterated forms and dried states (Susi et al., 1986).

341 FT-IR spectrum of native BSA (50 mg/mL) in water solution at ambient temperature is
342 shown in Figure 2A, in which the absorbance of IR radiation as a function of
343 wavenumber (in cm^{-1}) is reported. The protein structural units are able to absorb
344 specific wavelengths of radiation in the infrared region, giving rise to a characteristic set
345 of nine absorption bands, namely Amide A, B and Amide I-VII. Among them the amide
346 I and II represent the vibrational bands of the protein backbone (Krimm et al., 1986). In
347 particular, the absorption associated with the Amide I band takes into account the
348 stretching vibrations of the C=O bond (approximately 80%) of the amide groups, while
349 the Amide II band leads primarily to bending vibrations of the N—H bond (40–60% of
350 the potential energy) and CN stretching vibration (18–40%). Both the C=O and the N—
351 H bonds are involved in the hydrogen bonding between the different units of secondary
352 structure, and, accordingly, the locations of the Amide I and Amide II bands are
353 sensitive to the secondary structure content of a protein. Generally the analysis of FT-IR
354 spectra is restricted to the region of the Amide I bands, because, according to several
355 studies reported in the literature, Amide II band is not as good a predictor for
356 quantifying the secondary structure of proteins (Fabian et al. 2002; Kong & Yu, 2007;
357 Krimm et al., 1986; Murayama and Tomida, 2004; Surewicz & Mantsch, 1988).
358 According to the FT-IR spectrum shown in Figure 2A, the Amide I region is located in
359 the range between 1700 and 1600 cm^{-1} in agreement with the data reported in the
360 literature (Kong & Yu, 2007). The database, available in the literature and containing
361 the association between FT-IR peaks and secondary structure types, allows the
362 secondary structure of BSA to be defined through the analysis of the FT-IR spectra of
363 native protein and HHP treated samples. In order to narrow and separate the
364 intrinsically broad bands of the BSA spectrum, the second derivative analysis was
365 selected among the mathematical data analysis methods suitable to enhance the
366 resolution of the FT-IR spectrum.

367 The second derivative spectrum of BSA (50 mg/mL) at ambient pressure, shown in
368 Figure 2B, is dominated by four peaks at 1654, 1674, 1630, and 1610 cm^{-1} in the Amide
369 I region, in agreement with the studies of Murayama and Tomida (2004). The structure
370 of BSA protein is composed of 76% helix, 10% turns and 23% extended chain and no

371 beta (β) sheets (Fabian et al. 2002). The peak at 1654 cm^{-1} corresponds to α -helical
372 structures while the peak at 1674 cm^{-1} is associated with turn structures. Furthermore
373 the band at 1630 cm^{-1} is assigned to short-segment chains connecting to α -helix
374 segments of BSA and the one at 1610 cm^{-1} is due to the vibrations of glutaminy (Gln)
375 residues and the aromatic side chain, as already observed by Fabian et al. (2002).

376

377 **3.2.2 FT-IR spectra of HHP treated BSA**

378 Figure 3A and 3B and Figure 4A and 4B show the second derivative of the FT-IR
379 spectra of untreated BSA samples (50 and 100 mg/mL respectively) and treated at
380 different pressure levels (100-600 MPa) and treatment times (15-25 min) in the region
381 of the Amide I ($1600\text{-}1700\text{ cm}^{-1}$). As already observed for the samples of the native
382 BSA, the second derivative analysis clearly resolves the peaks of FT-IR spectra, which
383 can be associated to the secondary structure types, namely α -helix, β -sheets, random
384 coils and turns.

385 The second derivative spectrum of BSA samples (50 mg/mL) treated at high pressure
386 (200-600 MPa) for 15 minutes (Figure 5.4A) changes with the pressure level applied
387 and the holding time under pressure. BSA samples treated at 200 and 400 MPa show
388 two higher and broader peaks at 1645 and 1630 cm^{-1} , thus clearly indicating that high
389 pressure treatments are able to modify the secondary structure. In particular, in the case
390 of protein in water solution, the band between 1642 and 1624 cm^{-1} are assigned to α -
391 helix structure. At higher pressure levels, the changes in the secondary structure of BSA
392 become more relevant. Accordingly, the spectrum of BSA treated at 600 MPa for 15
393 minutes is characterized by a new peak at 1685 cm^{-1} , which can be associated with the
394 formation of intermolecular β -sheet aggregates.

395 Prolonged treatment times (25 min) enhance the effect of pressure, thus determining
396 higher differences among the spectra of the samples treated at different pressure level
397 (200, 400 and 600 MPa), as shown in Figure 3B. Furthermore, a more evident
398 occurrence of the peak at 1685 cm^{-1} is observed together with the occurrence of a new
399 peak at 1615 cm^{-1} associated with the formation of β -sheet intermolecular aggregates
400 (Lefevre et al., 2000). In particular, the 1685 cm^{-1} band correspond to antiparallel β -
401 sheet while the 1615 cm^{-1} band is due to the intermolecular β -sheets resulting from the
402 formation of molecular aggregates.

403 In more concentrated samples (Figure 4A and 4B), the spectra result more amplified in
404 the region between 1660-1630 cm^{-1} and a new peak at 1654 cm^{-1} associated with α -
405 helix structure is formed. At longer treatment times (Figure 4B) the α -helix structures
406 (1645 cm^{-1}) unfold into the disordered structure and turns, as demonstrated by the peak
407 at 1654 cm^{-1} . Also in this set of experiments, prolonged processing times enhance the
408 extent of molecular aggregation in protein secondary structure.

409

410 **3.3 Foaming properties**

411 Foaming capacity (FC%) of BSA samples with different concentration (50-100 mg/mL)
412 processed in high pressure treatments (100-600 MPa, 15-25 min) was evaluated and
413 compared to the foaming ability of the untreated samples. The experimental data are
414 shown in Figure 5A and 5B for the BSA sample with the concentration of 50 mg/mL
415 and 100 mg/mL, respectively.

416 According to the data shown in Figure 5A, HHP treatment is able to enhance the
417 foaming capacity of BSA, independently of the processing conditions. The values of
418 this functional properties increases with increasing the pressure level in the range
419 between 100 and 400 MPa, while a decreasing trend is detected at pressure level above
420 400 MPa. The dependence of the foaming ability on the pressure level, therefore,
421 follows the same trend already observed for the free SH groups, thus confirming BSA
422 partial unfolding in the pressure range between 100 and 400 MPa and the progressive
423 loss of the tertiary structure and the consequent polymerization of BSA protein in
424 dimers, trimers and higher oligomers held together by disulfide bonds.

425 The foaming properties, in fact, are mainly related to the protein capability to form film
426 at the air-water interface. The interfacial behavior of the protein, therefore, is strictly
427 controlled by the electrostatic and hydrophobic interactions as well as by the stability of
428 the disulphide bonds, which stabilize its secondary and tertiary structures. High pressure
429 disrupts hydrophobic interactions and ionic bonds resulting in protein molecules being
430 more suitable to adsorb air bubbles at air-water interface (Dickinson, 1989). This effect
431 is enhanced for the albumin proteins, which are amphiphilic molecules and are easy to
432 extend on the water-air interface (Li & Zhang, 2005; Yang et al., 2009). Similar results
433 are shown by Yang et al. (2009), who observed an increased foaming capability and
434 stability of egg white processed at pressure levels of 100-400 MPa. The authors
435 explained that HHP treatment reduced the hydrophobicity and solubility of the protein

436 and observed a positive correlation between the foaming capability and the surface
437 sulfhydryl content. The egg white samples exhibited greater foaming properties after a
438 HHP treatment at 350 MPa for 10 min.

439 The reduced foaming capacity observed for the protein samples treated with pressure
440 level above 400 MPa may be related to the irreversible unfolding, as demonstrated by
441 the reduction of the number of free SH-groups and FTIR spectra. Similarly Galaska et
442 al. (1997) observed a reduction in surface hydrophobicity of pure BSA in solution
443 (pH=7) processed with pressure level between 400 and 800 MPa. The authors attributed
444 the loss of surface hydrophobicity to the partial unfolding and the intermolecular
445 association of BSA protein after pressure release. Moreover, as the increase of the
446 pressure levels enhances the formation of aggregates the foaming ability of the samples
447 decreases.

448 Similarly, Krešić et al. (2006) observed that high-pressure treatments (300 MPa and 600
449 MPa, for 5 and 10 min) significantly improved the foaming capacity of WPI and WPC
450 due to the protein unfolding. A decrease of the foaming volume (FV) was detected if
451 processing pressure was higher than 600 MPa because of the loss in protein solubility
452 occurring at very high pressures. A significant reduction of the solubility of whey
453 proteins after pressurization was also observed by Pittia et al. (1996). Van der Plancken
454 et al. (2006) investigated the effect of a combined process of high pressure (400-700
455 MPa) and heating (50-85 °C) on foaming properties of egg white solutions. The authors
456 observed an increase in foaming ability of those samples with high extent of unfolding
457 and residual solubility with the best stability and volume foam reached at pH 8.8 above
458 500 MPa. The authors reported the association between foaming ability and protein
459 flexibility/solubility and noticed an increase in foaming ability at higher exposed SH
460 content (Van der Plancken et al., 2006).

461 If the effect of the processing time is considered, foaming ability was clearly higher in
462 samples treated for a shorter processing time (15 min). Prolonged processing times (25
463 min) promote a larger extent of aggregation which prevent the formation of protein
464 foams. A similar mechanism can explain the effect of protein concentration in the
465 processed samples. If the results shown in Figure 5A and 5B are compared, the foaming
466 ability decreases with the protein concentration in the processed samples. Protein
467 concentration in solution controls the extent of protein-protein interaction, this allowing
468 the formation of small aggregates at lower pressure level.

469 **3.4 Emulsifying properties**

470 The emulsifying properties are generally recognized as the most important parameters
471 among the functional properties and used to determine the degree of protein
472 denaturation and aggregation.

473 Figure 6 shows the values of the EAI (m^2/g) of BSA samples with different
474 concentration (50-100 mg/mL) processed in high pressure treatments (100-600 MPa,
475 15-25 min).

476 The EAI is a measure of the interfacial area stabilized per unit weight of protein and
477 represents the protein capacity to stay at the water/oil interface after the emulsion
478 formation (Boye et al., 2010). The dependence of EAI values on the processing pressure
479 varies with protein concentration, as already observed for the free-SH groups and the
480 foaming capacity. In BSA sample with a concentration of 50 mg/mL, the emulsifying
481 activity index increases with the processing pressure in the range between 100 and 400
482 MPa, while at higher pressure level a slight decrease in the EAI values can be observed.
483 Prolonged processing times (25 min) still contribute to enhance the emulsifying
484 capacity of the HHP treated protein solutions. In BSA sample with a concentration of
485 100 mg/mL, the EAI values follow a different trend. For shorter processing times (15
486 min), the EAI values are higher than the one measured for the control samples and
487 almost independent on the processing pressure. The BSA samples processed for 25 min,
488 instead, show a significant decrease in the EAI values at pressure level above 300 MPa
489 ($p < 0.05$). When the pressure levels is above 400 MPa, the BSA samples show
490 significantly lower ($p < 0.05$) EAI values than that of untreated one. As already observed
491 for the foaming capacity, the observed variation of the emulsifying property could be
492 due to the unfolding of proteins and subsequent loss of protein solubility. Thus, the
493 proteins could not adsorb at the water/oil interface when they were insolubilized and
494 aggregated.

495 Figure 7 shows the values of the ESI (%) of BSA samples with different concentration
496 (50-100 mg/mL) processed in high pressure treatments (100-600 MPa, 15-25 min. ESI
497 provides a measure of the ability of protein to stabilize the structure of the emulsion
498 over a defined period of time (Boye et al., 2010). According to the experimental data
499 shown in Figure 7A, the HHP treatments enhance the stability of the protein/oil
500 emulsion in the pressure range between 100 and 400 MPa for the sample processed for
501 15 min and in the pressure range between 100 and 300 MPa for the sample processed

502 for 25 min. Pressure levels above the mentioned range determine a significant decrease
503 in the ESI values ($p < 0.05$), which are, in any case, higher than the ones measured for
504 the untreated samples. If the protein concentration increases (Figure 7B), the ESI values
505 estimated for the samples processed for 15 min are almost stable and not-significantly
506 different ($p > 0.05$) from the values of the untreated samples, if the processing pressure is
507 lower than 400 MPa. At pressure level above 400 MPa, the HHP treatments enhance the
508 stability of the protein/oil emulsion. An opposite trend can be observed for the samples
509 treated for 25 min, showing ESI values decreasing with the processing pressure above
510 400 MPa. This effect may result from a decline in molecular flexibility of the proteins
511 because of protein aggregation, since molecular flexibility is an important factor
512 influencing emulsion stability (Tang et al., 2005). According to the mechanism of the
513 emulsification process proposed by Tang et al. (2005), it consists of at least three steps:
514 the adsorption of protein on the O/W interface; the changes of quaternary and tertiary
515 conformations; the formation of a stable viscoelastic film. The first step is clearly
516 affected by protein solubility and highly dependent on the flexibility in quaternary
517 conformation. The occurrence of protein unfolding under pressure and the consequent
518 modification of the tertiary structure affect the emulsion stability, clearly influencing
519 the second and the third step of the emulsification process.
520 Moreover protein concentration influences the stability of the protein/oil emulsions,
521 thus determining lower values of the ESI at higher protein concentration and confirming
522 the formation of small aggregates.

523

524 3.5 Correlation analysis

525 Correlations between the functional parameters and the content of free SH-groups of
526 BSA samples as affected by HHP treatments were summarized in Table 1. The data still
527 confirm the observation reported in the previous paragraphs. For the BSA samples with
528 a concentration of 50 mg/mL processed for 15 min, the whole analyzed parameters
529 show a strong positive correlation, while at prolonged processing times, only the
530 number of free SH-groups has a strong positive correlation with the foaming capacity,
531 the ESA and ESI values. Moreover the correlation between ESI values and ESA or FC
532 value becomes moderate. For the samples with a concentration of 100 mg/mL for 15
533 min, instead, a strong positive correlation exists between the number of free SH-groups
534 and the ESA values, as well as between the foaming capacity and the ESA; positive or

535 negative moderate correlations are detected for the other analyzed parameters. At longer
536 processing times, the positive strong correlations are replaced by very weak or weak
537 correlations (negative and positive), thus demonstrating that different mechanisms
538 control the effect of HHP treatment on the analyzed parameters.

539

540 **4. Conclusions**

541 High Hydrostatic Pressure resulted in protein unfolding and/or aggregation of proteins
542 showing the potential to induce changes in BSA structure as well as in its functional
543 properties. Protein unfolding occurs in the pressure range, which depends on protein
544 concentration and treatments time. In the unfolded state, BSA proteins show improved
545 foaming properties, expose a higher number of SH free groups and are characterized by
546 negligible modifications of the secondary structure. Pressure levels above the threshold
547 valued, prolonged processing times and/or high protein concentration allow the
548 polymerization of BSA protein in dimers, trimers and higher oligomers held together by
549 disulfide bonds, as demonstrated by the reduction of foaming and emulsifying
550 properties and the significant changes in secondary structure detected.

551 The experimental results demonstrated so far that the effect of HHP treatments on
552 protein structure may be predicted through a proper selection of both protein
553 concentration and process conditions. The availability and reactivity of free SH groups
554 represent the key factor controlling the mechanism of HHP action on proteins and
555 determining the functional properties as well as the stability of the proteins in solution,
556 in a certain range of protein concentration. Protein concentration, indeed, in solution
557 controls the extent of protein-protein interaction, as demonstrated by the variation of the
558 functional properties and the secondary structure of the HHP treated proteins.

559 **References**

- 560 1. Ahmed, J., Ramaswamy, H. S., Kasapis, S., & Boye, J. I. (2010). Novel food
561 processing: effects on rheological and functional properties. Boca Raton: CRC,
562 226–229.
- 563 2. Barba, F. J., Esteve, M. J., & Frigola, A. (2012). High pressure treatment effect on
564 physicochemical and nutritional properties of fluid foods during storage: a review.
565 *Comprehensive Reviews in Food Science and Food Safety* **11**, 307–322.
- 566 3. Beveridge, T., Toma, S. J., & Nakai, S. (1974). Determination of SH groups and SS
567 groups in some food proteins using Ellmans reagent. *Journal of Food Science* **39**,
568 49–51.
- 569 4. Boye, J.I., Aksay, S., Roufik, S. et al. (2010). Comparison of the functional
570 properties of pea, chickpea and lentil protein concentrates processed using
571 ultrafiltration and isoelectric precipitation techniques. *Food Research International*,
572 43, 537–546.
- 573 5. Buchow, R. Wendorff, J., Hemar, Y. (2011). Conjugation of Bovine Serum
574 Albumin and Glucose under Combined High Pressure and Heat. *Journal of*
575 *Agriculture and Food Chemistry* **59**, 3915–3923.
- 576 6. Cameron, D.R., Weber, M.E., Idziak, E.S., Neufeld, R.J. And Cooper, D.G. (1991).
577 Determination of interfacial areas in emulsions using turbidimetric and droplet size
578 data: Correction of the formula for emulsifying activity index. *Journal of*
579 *Agriculture and Food Chemistry* **39**, 655–659.
- 580 7. Cheftel, J.L., Cuq, J.L., Lorient, D. (1985). *Protéines Alimentaries*. pp:58-65. Paris:
581 Techniques et documentation Lavosier.
- 582 8. Cheftel, J. (1992). Effects of high hydrostatic pressure on food constituents: An
583 overview. *High Pressure and Biotechnology* **224**, 195-209.
- 584 9. Denda A., & Hayashi, R. (1992). Emulsifying properties of pressure treated
585 proteins. In C. Balny, R. Hayashi, K. Heremans, & P. Masson, *High pressure and*
586 *biotechnology*”. (pp. 211-218), vol. 224. Montrouge: Libbey Eurotext Ltd.
- 587 10. Dickinson, E. (1989). Protein adsorption at liquid interfaces and the relationship to
588 foam stability. In A. J. Wilson, *Foams: physics, chemistry and structure* (pp. 39-53).
589 London: Springer.

- 590 11. Fabian H, Mantsch HH. (1995). Ribonuclease A revisited: Infrared spectroscopic
591 evidence for lack of native-like secondary structures in the thermally denatured
592 state. *Biochemistry* **34**, 13651–13655.
- 593 12. Fabian, H., and Mantele, W. (2002). Infrared Spectroscopy of Proteins, in
594 Handbook of Vibrational Spectroscopy. Vol. 5, pp 3999-3424, John Wiley and
595 Sons, Chichester.
- 596 13. Galazka, V. B., Dickinson, E., & Ledward, D. A. (2000). Influence of high pressure
597 processing on protein solutions and emulsions. *Current Opinion in Colloid &*
598 *Interface Science* **5** (3–4), 182–187.
- 599 14. Gross, M. & Jaenicke, R. (1994). Proteins under pressure. The influence of high
600 hydrostatic pressure on structure, function and assembly of proteins and protein
601 complexes. *European Journal of Biochemistry* **221**, 617-630.
- 602 15. Hardham, J. F. (1981). The determination of total and reactive sulphhydryl of whey
603 protein concentrates. *The Australian Journal of Dairy Technology* **36** (4), 153–155.
- 604 16. Hammershøj M., Larsen L.B. (1999). Foaming of ovalbumin and egg albumen
605 fractions and the role of the disulfide bonds at various pH levels. In: Cavalchini
606 G.C., Baroli D. (eds): Proceeding of VII European Symposium on the Quality of
607 Eggs and Egg Products. Bologna, 19–23 September: 351–357.
- 608 17. Ibanoglu, E., Karatas, S. (2001). High pressure effect on foaming behaviour of whey
609 protein isolate. *Journal of Food Engineering* **47**, 31-36.
- 610 18. Kato, A.; Ibrahim, H.R.; Watanabe, H.; Honma, K.; Kobayashi, K. (1989). New
611 approach to improve the gelling and surface functional properties of dried egg white
612 by heating in dry state. *Journal of Agricultural and Food Chemistry* **37**, 433-437.
- 613 19. Kong J., bYu, S. (2007). Fourier Transform Infrared Spectroscopic Analysis of
614 Protein Secondary Structures. *Acta Biochimica et Biophysica Sinica* **39** (8), 549–
615 559.
- 616 20. Knorr, D., Bottcher, A., Dornenburg, H., Eshtiaghi, M., Oxen, P., Richwin, A., &
617 Seyderhelm, I. (1992). High pressure effects on microorganisms, enzyme activity
618 and food functionality. In C. Balny, R. Hayashi, K. Heremans, & P. Masson, High
619 pressure and biotechnology (pp. 211-218), vol. 224. Montrouge: Libbey Eurotext
620 Ltd.

- 621 21. Kresic G., Lelas V., Herceg, Z., Rezec, A. (2006). "Effects of high pressure on
622 functionality of whey protein concentrate and whey protein isolate". *Lait*, **86**, 303-
623 315.
- 624 22. Krimm, S., Bandekar, J. (1986). Vibrational spectroscopy and conformation of
625 peptides, polypeptides, and proteins. *Advance in Protein Chemistry* **38**, 181–364.
- 626 23. Lefevre, T. & Subirade, M. (2000). "Molecular differences in the formation and
627 structure of fine-stranded and particulate α -lactoglobulin gels". *Biopolymers* **54**, 578-
628 586.
- 629 24. Li-Chan, E., Nakai, S. (1989). "Biochemical basis for the properties of egg white.
630 *Critical Reviews in Poultry Biology* **2**, 21-57.
- 631 25. Lomakina K., Míková K. (2006). A Study of the factors affecting the foaming
632 properties of egg white-a review. *Czech Journal Food Science*, **24**, 110–118.
- 633 26. Martelli, M., De Chiara, A., Corvo, M., Restani P., Fiocchi, A. (2002). Beef Allergy
634 in Children with Cow's Milk Allergy; Cow'S Milk Allergy in Children with Beef
635 Allergy. *Annals of Allergy, Asthma and Immunology* **89**(6), 38-43.
636 doi:10.1016/S1081-1206(10)62121-7
- 637 27. Monahan, F.J., German, J.B., Kinsellat, J.E. (1995). Effect of pH and Temperature
638 on Protein Unfolding and Thiol/Disulfide Interchange Reactions during Heat-
639 Induced Gelation of Whey Proteins. *Journal of Agriculture and Food Chemistry* **43**,
640 46-52.
- 641 28. Murayama, K. & Tomida, M. (2004). Heat-Induced Secondary Structure and
642 Conformation Change of Bovine Serum Albumin Investigated by Fourier Transform
643 Infrared Spectroscopy. *Biochemistry* **43**, 11526-11532.
- 644 29. Pearce, K.N. And Kinsella, J.E. (1978). Emulsifying properties of proteins:
645 Evaluation of a turbidimetric technique. *Journal of Agriculture and Food Chemistry*
646 **26**, 716–723.
- 647 30. Penãs, E., Prestamo, G., Baezac, M. L., Martinez-oleroc, M. I., Gomez, R. (2006).
648 Effects of combined high pressure and enzymatic treatments on the hydrolysis and
649 immunoreactivity of dairy whey proteins. *International Dairy Journal* **16**, 831–839.
- 650 31. Pittia, P., Wilde, P. J., Husband, F. A., & Clark, D. C. (1996). Functional and
651 structural properties of b-lactoglobulin as affected by high pressure treatment.
652 *Journal of Food Science* **61**, 1123-1128.

- 653 32. Quin, Z., Guo, X., Lin, Y., Chen, J., Liao, X., Hu, X., et al. (2012). Effects of high
654 hydrostatic pressure on physicochemical and functional properties of walnut
655 (*Juglans regia* L.) protein isolate. *Journal of the Science of Food and Agriculture*.
656 DOI: 10.1002/jsfa.5857.
- 657 33. Shriver, S.K. and Yang, W.W. (2011). Thermal and Nonthermal Methods for Food
658 Allergen Control. *Food Engineering Reviews*, 3, 26-43.
- 659 34. Silva, J.G., Morais, H.A. And Silvestre, M.P.C. (2003). Comparative study of the
660 functional properties of bovine globulin isolates and sodium caseinate. *Food*
661 *Research International* **36**, 73–80.
- 662 35. Speroni, F., Beaumal, V., de Lamballerie, M., Anton, M., Anon, M. C., & Puppo,
663 M. C. (2009). Gelation of soybean proteins induced by sequential high-pressure and
664 thermal treatments. *Food Hydrocolloids* **23**, 1433–1442.
- 665 36. Susi, H. & Byler, D.M. (1986). Resolution-enhanced Fourier transform infrared
666 spectroscopy of enzyme. *Methods Enzymology* **130**, 290-311.
- 667 37. Tang C. H., Yang, X.Q., Chen, Z., Wu, H., Peng Z.w. (2005). Physicochemical and
668 structural characteristics of Sodium Caseinate biopolymers induced by microbial
669 Transglutaminase. *Journal of Food Biochemistry* 29, 402–421.
- 670 38. Tang, C. H., & Ma, C. Y. (2009). Effect of high pressure treatment on aggregation
671 and structural properties of soy protein isolate. *LWT–Food. Science and Technology*
672 **42**, 606–611.
- 673 39. Tauscher, B. (1995). Pasteurization of food by hydrostatic high pressure: chemical
674 aspects. *Zeitschrift fur Lebensmittel Untersuchung und –Forschung* **200**, 3–13.
- 675 40. Van der Plancken, I., Van Loey, A., Hendrickx, ME. (2005). Changes in sulfhydryl
676 content of egg white proteins due to heat and pressure treatment. *Journal of*
677 *Agriculture and Food Chemistry* **53** (14), 5726-5733.
- 678 41. Yang R.X., Li W.Z., Zhu C.Q, Zhang Q. (2009). Effects of ultra-high hydrostatic
679 pressure on foaming and physical-chemistry properties of egg white. *Journal of*
680 *Biomedical Science and Engineering* **2**, 617-620.
- 681 42. Yang R.X., Qiao, L., Gu, X., Li, J., Xu,R. Wang, M., Reuhs, B., Yang, Y. (2010).
682 Effect of high pressure treatment on the physicochemical and functional properties
683 of egg yolk. *European Food Research Technology* **231**, 371–377.
- 684

685 **Figure Captions**

686

687 **Figure 1** Free SH-groups in BSA samples processed in HHP treatments at different
688 pressure levels (100-600 MPa) and processing times (15 min, 25 min). **A:** protein
689 concentration of 50 mg/mL; **B:** protein concentration of 100 mg/mL.

690

691 **Figure 2** FT-IR Spectra of BSA (50 mg/mL) native protein at 25 °C. **A:** FT-IR
692 spectrum; **B:** Second derivative spectrum of the Amide I.

693

694 **Figure 3** FT-IR Spectra of BSA (50 mg/mL) samples processed in HHP treatments at
695 different pressure levels (100-600 MPa). **A:** treatment time=15 min; **B:** treatment
696 time=25 min.

697

698 **Figure 4** FT-IR Spectrum of BSA (100 mg/mL) samples processed in HHP treatments
699 at different pressure levels (100-600 MPa). **A:** treatment time=15 min; **B:** treatment
700 time=25 min.

701

702 **Figure 5** Foaming ability of BSA samples processed in HHP treatments at different
703 pressure levels (100-600 MPa) and processing times (15 min, 25 min). **A:** protein
704 concentration of 50 mg/mL; **B:** protein concentration of 100 mg/mL.

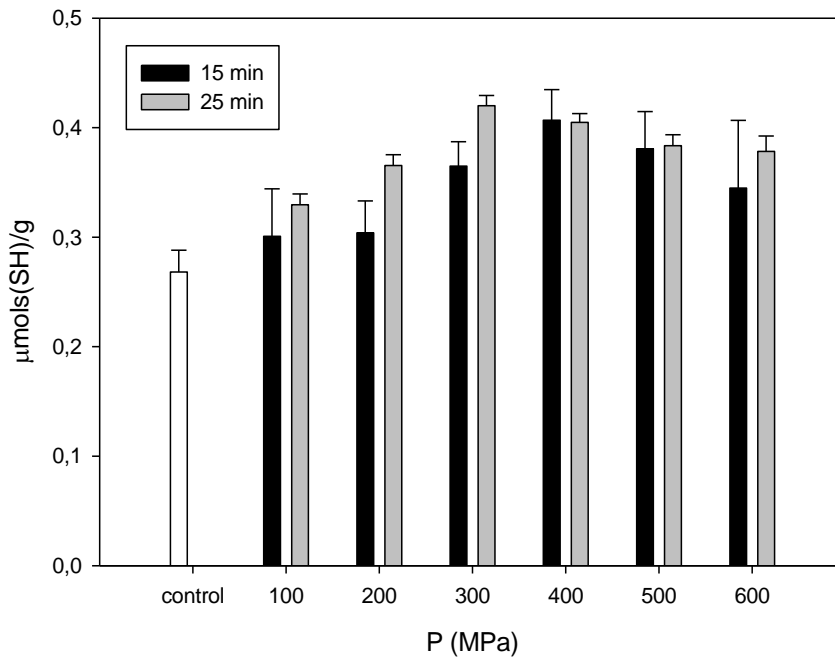
705

706 **Figure 6** Emulsion Ability Index (EAI) of BSA samples processed in HHP treatments
707 at different pressure levels (100-600 MPa) and processing times (15 min, 25 min). **A:**
708 protein concentration of 50 mg/mL; **B:** protein concentration of 100 mg/mL.

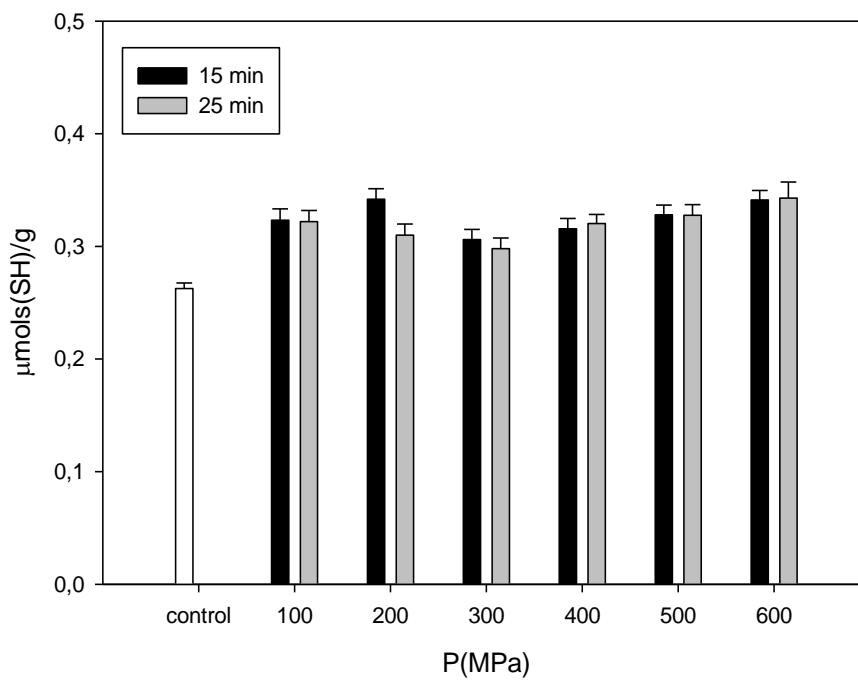
709

710 **Figure 7** Emulsion Stability Index (ESI) of BSA samples processed in HHP treatments
711 at different pressure levels (100-600 MPa) and processing times (15 min, 25 min). **A:**
712 protein concentration of 50 mg/mL; **B:** protein concentration of 100 mg/mL.

713 **Figure 1**
714
715 **A**

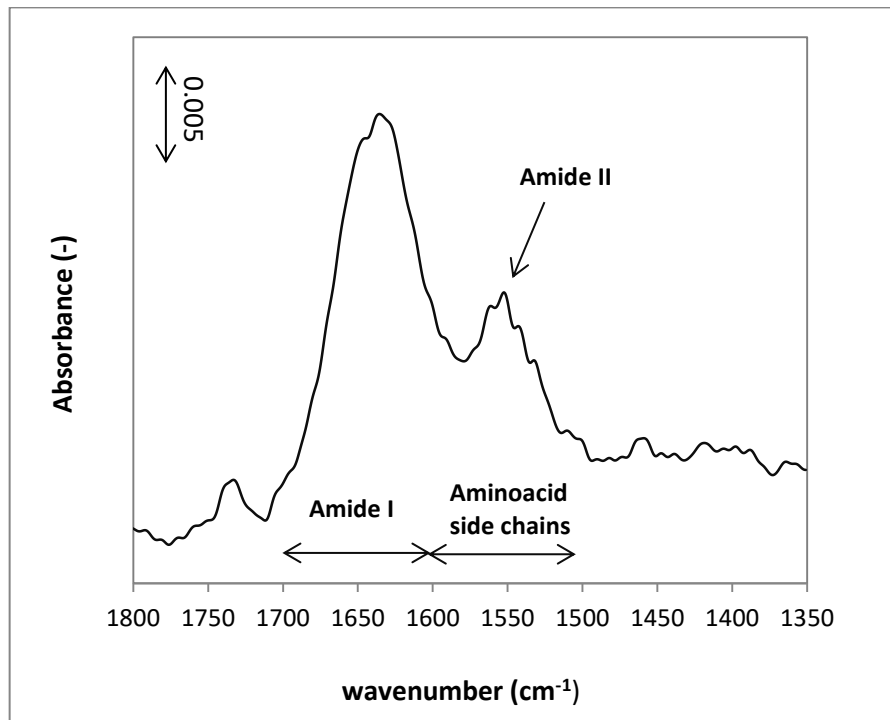


716
717
718 **B**

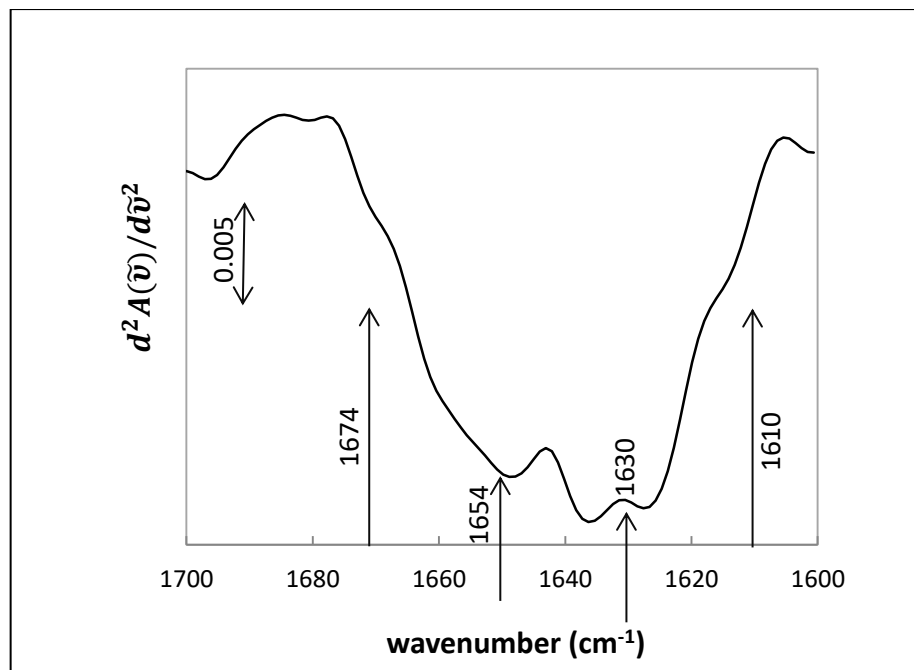


719
720

721 **Figure 2**
722
723 **A**
724



725
726
727 **B**
728



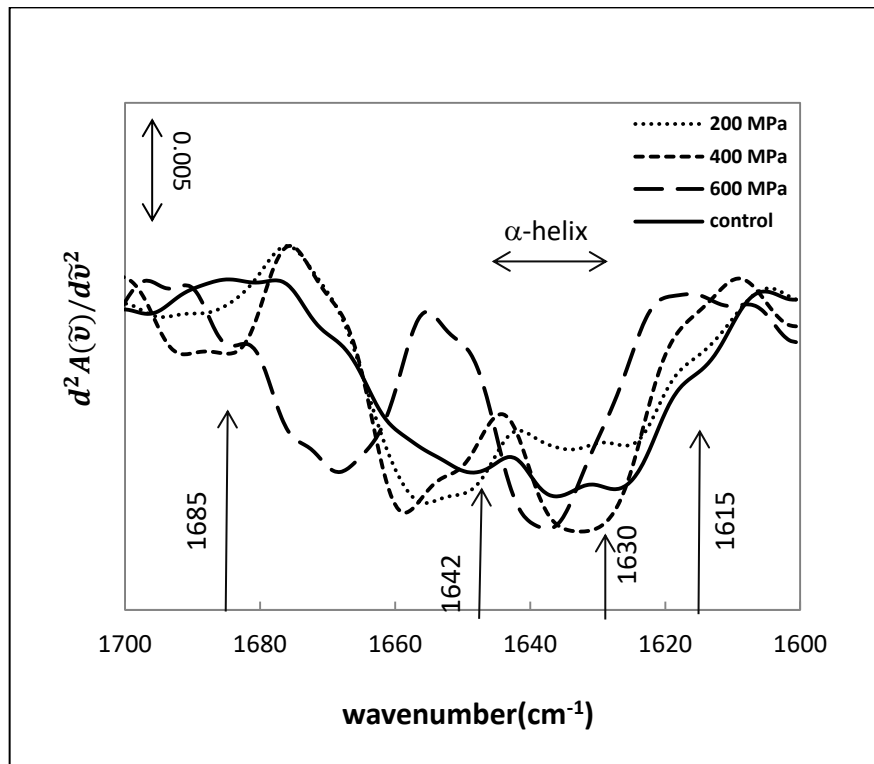
729
730
731
732
733

734 **Figure 3**

735

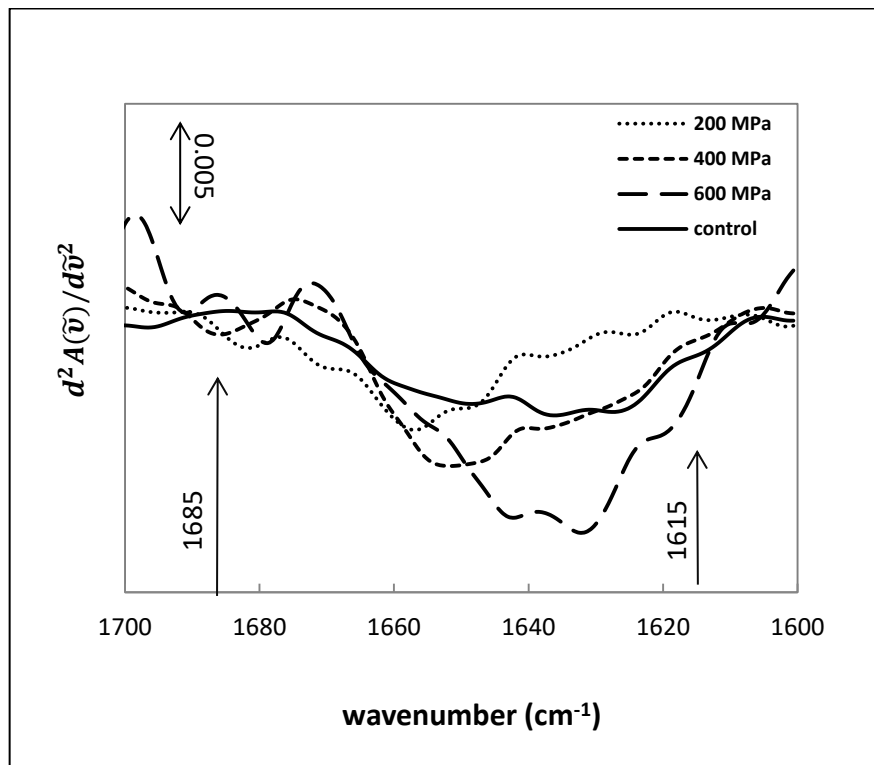
736

737 **A**



738

739 **B**



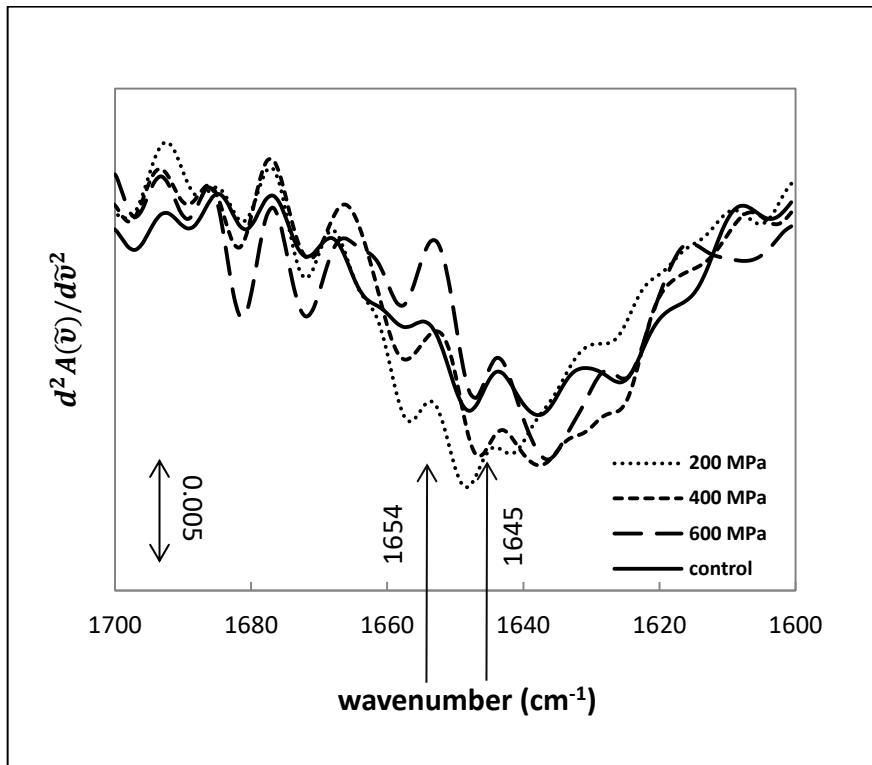
740

741

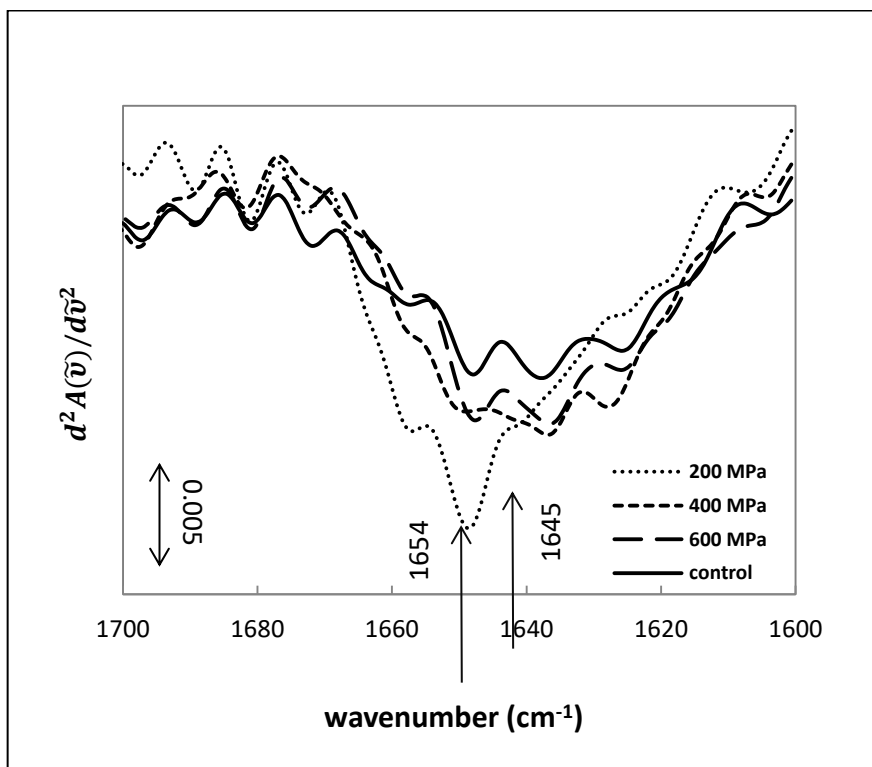
742

743

744 **Figure 4**
745 **A**
746



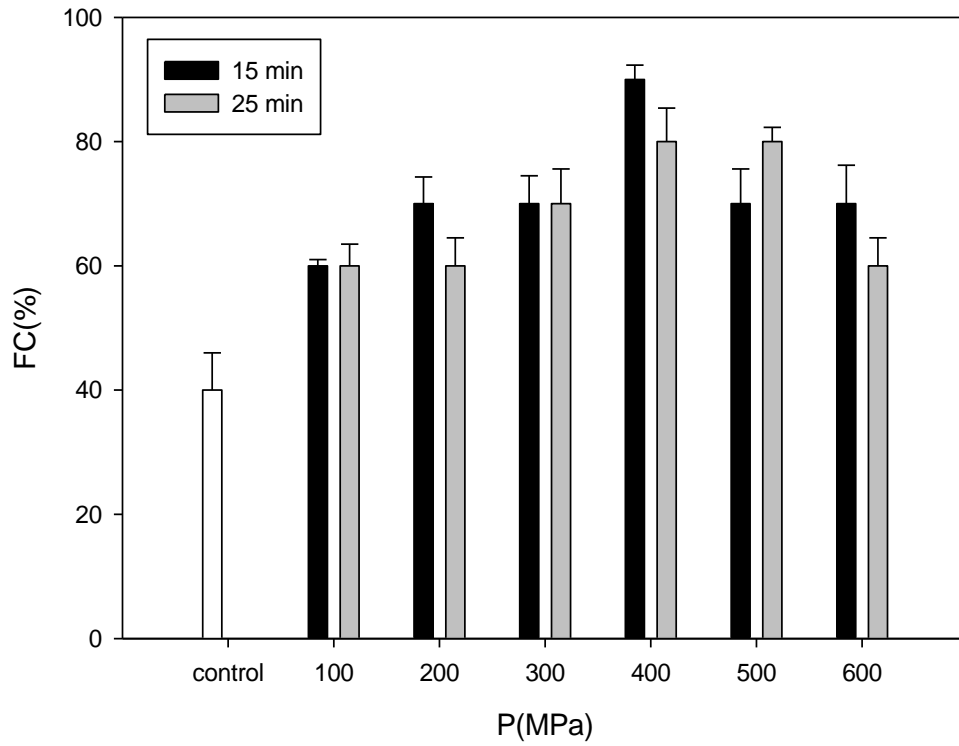
747 **B**
748
749



750
751
752
753

754 **Figure 5**

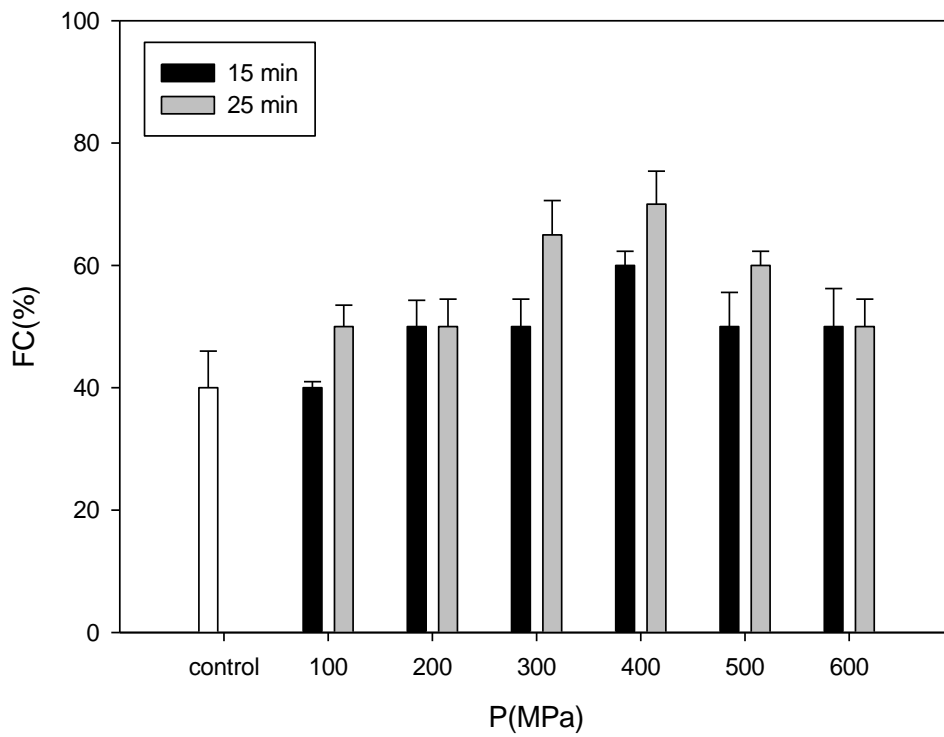
755 **A**



756

757 **B**

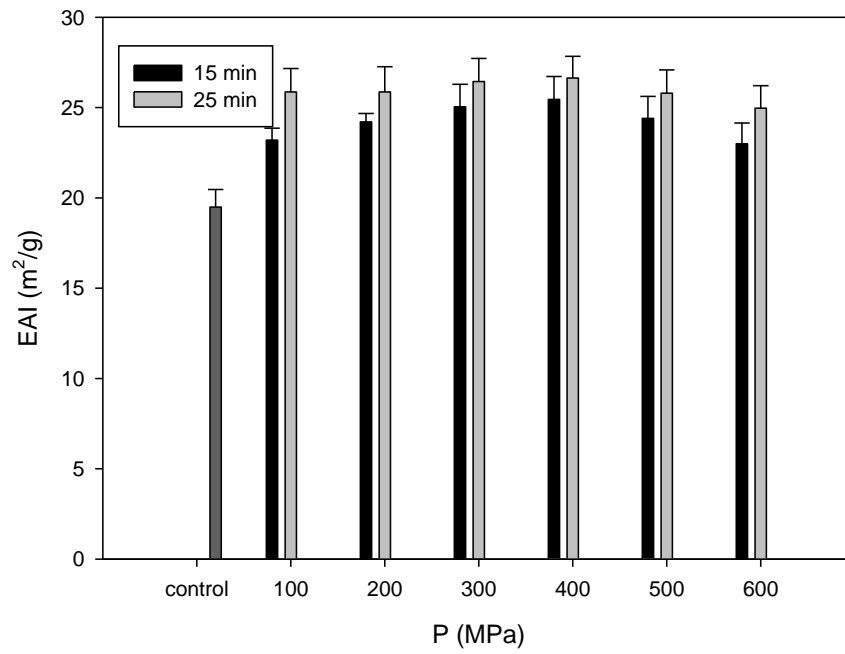
758



759

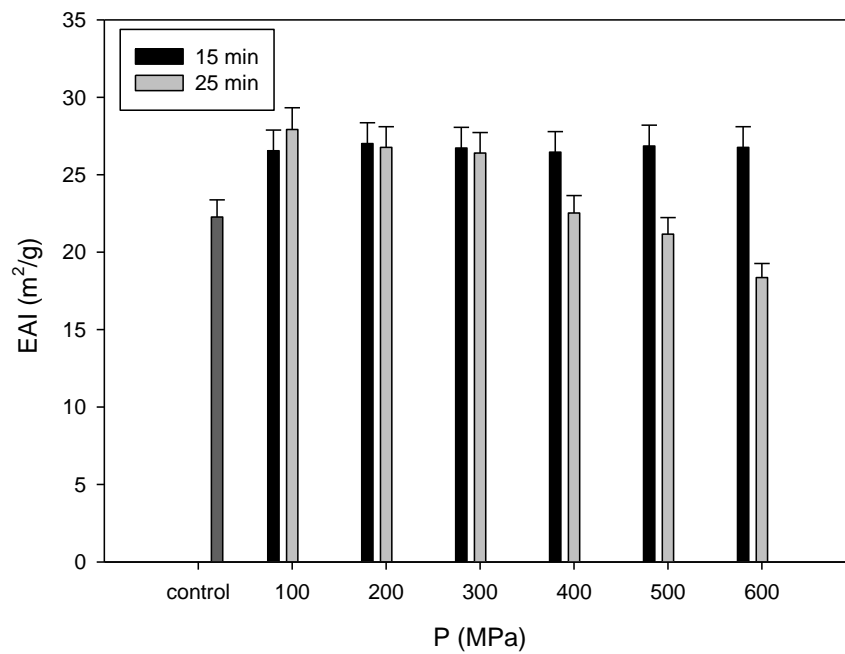
760 **Figure 6**

761 **A**



762

763 **B**

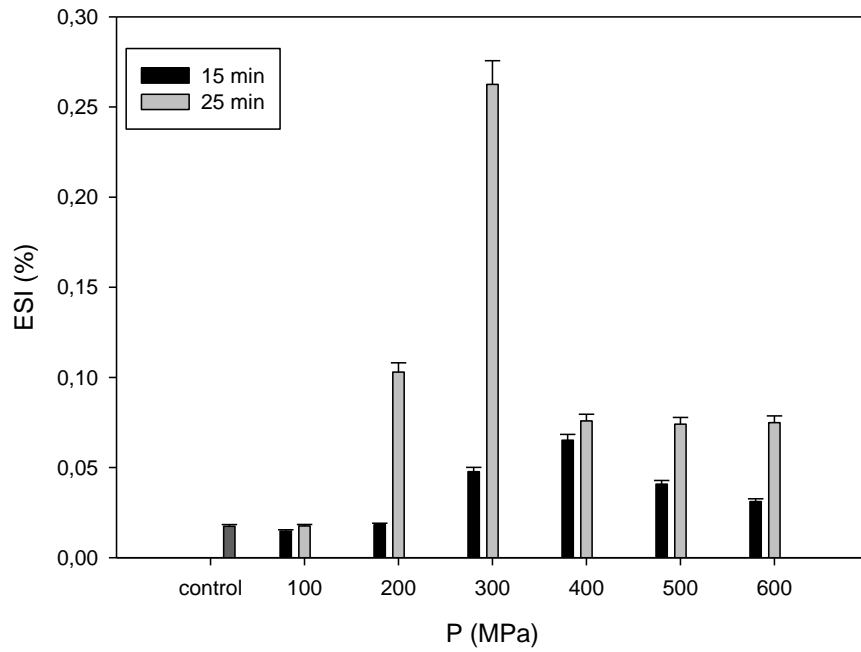


764

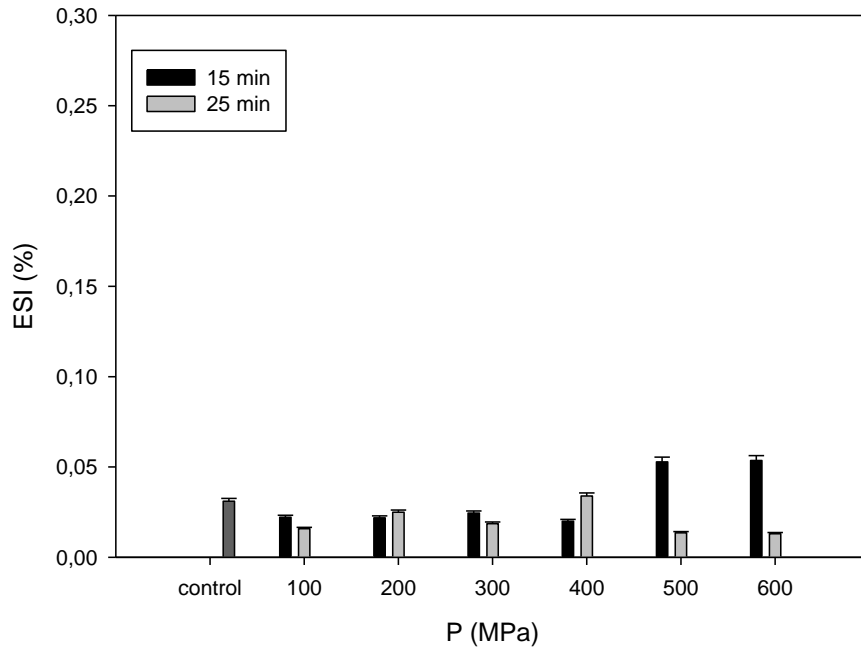
765

766 **Figure 7**

767 **A**



768 **B**



770

771

772 **Table captions**

773

774 **Table 1** Correlations among functional properties and the content of free SH- groups of

775 BSA samples processed in HHP treatments at different pressure levels (100-600 MPa)

776 and processing times (15 min, 25 min). A: protein concentration of 50 mg/mL; B:

777 protein concentration of 100 mg/mL.

778

779 **Table 1**

780 **A**

Processing time: 15 min				
	SH	FC	ESA	ESI
SH		0,866	0,805	0,921
FC	0,866		0,910	0,723
ESA	0,805	0,910		0,613
ESI	0,921	0,723	0,613	
Processing time: 25 min				
	SH	FC	ESA	ESI
SH		0,855	0,634	0,708
FC	0,855		0,547	0,373
ESA	0,634	0,547		0,348
ESI	0,704	0,374	0,348	

781

782 **B**

Processing time: 15 min				
	SH	FC	ESA	ESI
SH		0,273	0,906	0,244
FC	0,273		0,593	-0,158
ESA	0,906	0,593		0,074
ESI	0,244	-0,158	0,074	
Processing time: 25 min				
	SH	FC	ESA	ESI
SH		0,444	-0,270	-0,591
FC	0,444		-0,2793	0,245
ESA	-0,270	-0,280		0,089
ESI	-0,591	0,245	0,089	

783